UNIVERSITI TEKNOLOGI MARA

MATHEMATICS AND STATISTICS

UNDERGRADUATE RESEARCH PROCEEDINGS 2025

UiTM CAWANGAN NEGERI SEMBILAN

NUMERICAL SOLUTION OF NANOFLUID FLOW OVER A PERMEABLE STRETCHING AND SHRINKING SURFACE USING BVP4C SOLVER

(exactly 12 pt)

Nurqasrina Ahmad Azian[1,*], Siti Hidayah Muhad Saleh[2]

[1]*College of Computing, Informatics and Mathematics, Universiti Teknologi MARA, Kampus Seremban, Negeri Sembilan*

[*]qasrina.azian02@gmail.com

Abstract

This study investigates nanofluid flow over a permeable stretching/shrinking surface using BVP4C. This study utilises copper and silver nanoparticles to examine how well the two nanoparticles transfer heat. The aim of this study is to apply the similarity transformation to convert the partial differential equation (PDE) to an ordinary differential equation (ODE). The objective is to solve nanofluid flow over a permeable stretching/shrinking surface by using BVP4C. BVP4C in MATLAB software is then used to solve this equation numerically. The study then compares the results between the previous method which is the shooting method , and BVP4C, thus identifying the impact of copper and silver nanoparticles on the stretching/shrinking surface that influence the efficiency of heat transfer by analysing and measuring the nanoparticles in velocity profile, temperature profile, skin friction coefficient and local Nusselt number. The comparison demonstrates strong agreement between the computed skin friction coefficient and local Nusselt number obtained using BVP4C. The obtained result indicates that in the stretching case, the velocity profile, temperature profile, and boundary layer thickness decrease, but in the shrinking case, the velocity profile, temperature profile, and boundary layer thickness increase. In addition, the skin friction coefficient of silver is higher than that of copper, which contributes to a decrease in the velocity boundary layer. Meanwhile, the local Nusselt number of silver nanoparticles are higher than that of copper, indicating a higher rate of heat transfer for silver.

Keywords*:* Nanofluid, stretching/shrinking surfaces, permeable, BVP4C

1. Introduction

The concept of nanofluid emerged with the intention of improving the fluid's thermal conductivity, which encouraged advancements in a range of engineering sectors. The discovery of heat transmission fluids like air, ethylene glycol, water, and oil have extremely poor thermal conductivity compared to solids. The idea of renewal led to developing the electrical conductivity of heterogeneous solid particles and allowed the study of the conductivity of a mixture of liquid and solid particles to increase thermal conductivity [1]. The purpose of nanofluid remains the same intent of emphasising the improvement of thermal characteristics to the new technology specifically, nanotechnology in order to attain the greatest possible thermal conductivity. A permeable surface is a surface with holes or boundaries that let fluid

pass through or be absorbed. The surface has the ability for the fluid to be suction or injected into the boundary layer of the surface. Suction is a method used to manage flow and modify turbulence induced by flow instability downstream of the boundary layer separation point [2]. The fluid flow over a permeable surface is commonly used in engineering applications, including air foil design, filtration systems, and combustion chambers.

Next, the structure of the boundary layer, which is defined as a light layer of gas or liquid that touches an object's surface, is affected by the existence of suspended nanoparticles in the general fluid. Permeable surface and boundary layer have a significant influence on heat transfer [3]. Heat transmission rates are enhanced when fluid is removed from the boundary layer because convective processes are more efficient [4]. While an injection of the surface will reduce the transmission of heat since the heat of the surface has dropped due to the additional fluid. Therefore, heat transmission is a basic thermodynamic and engineering concept that describes the motion of the heat energy from one system to another as due to temperature differences. Conduction, convection, and radiation are the three primary processes in heat transmission with different circumstances. In addition, this research uses copper and silver as a nanoparticle to study the impact on the transfer of heat and fluid flow. Several studies have established that nanofluids provide an effective way of conveying thermal conductivity and heat.

The impact of surface roughness on mixed convective nanofluid flow across an exponentially extending permeable surface using the quasilinearization technique has been conducted by [5]. The research findings conclude that nanoparticles in the base fluid have been significantly affected by its flow since it increases friction around walls and reduces heat transfer from hot to cold fluid. The study made by [6] for nanofluid flow past a nonlinearly stretching surface with shear flow and zero nanoparticle flux by the shooting method, indicated that the injection surface will affect temperature drops and wall shear stress and decrease in heat transfer speed. The velocity of fluid reduced when the nonlinear stretching parameter was amplified. The Prandtl number helps in cooling in a variety of systems when the heat of boundary layer width decreases. The numerical solution of nanofluid flow over permeable stretching and shrinking surfaces has been well researched. From the previous study, nanofluids exhibit superior thermal conductivity compared to base fluids, enhancing the rate of heat transfer between solid particles and the base fluid due to increased surface area [1].

The study of [7] stated that the heat transfer rate increases with heat radiation. Boundary layer separation was delayed by suction parameter growth while the increase in volume amount of hybrid nanofluids (copper and alumina) provides superior heat transport compared to nanofluids and water. While research by [8] studied about examining how TiO2-Ag/water affects hybrid nanofluid MHD flow while taking radiation and slip conditions into account across exponentially expanding and contracting sheets by using the BVP4C method. The research concludes that the presence of the nanoparticles raises the temperature. When the velocity slip parameter was raised, the skin-friction coefficient reduced in the $\lambda < 0$ shrinking surface region but contradiction was seen on the $\lambda > 0$ stretching surface, while the Nusselt number had the opposite impact. On the other hand, the results showed that increases in skin friction and Nusselt number were influenced by the volume of nanoparticles and the heat

transfer rate when a general nanofluid was transformed into a hybrid nanofluid by raising its viscosity. Higher skin friction coefficient and velocity gradient are the results of increased instability parameters [9].

The study of a three-dimensional unsteady radiative hybrid nanofluid flow over a permeable surface through a porous space by the BVP4C method concludes that the increase in heat transfer rate has the potential to decrease shrinking capacity, while excessive surface shrinking might raise the Skin Friction Coefficient [2]. Hence, the study of the rate of heat transfer rises as a result of an unstable hybrid nanofluid flow across a radially permeable shrinking/stretching surface, depending on the mass suction parameter and the volume percentage of nanoparticles [10]. Lastly, the research on the effect of radiation from heat and suction effect the unstable ternary mixed nanofluid flow across a biaxial shrinking sheet indicates that shows that raising the suction parameter in ternary innovative hybrid nanofluids generates improvement in local skin friction and a delay in boundary layer separations. Boundary layer separation was not significantly influenced by thermal radiation. Higher velocities and a lower system temperature are the results of increased suction. While thermal radiation at high intensities significantly increases the ternary hybrid nanofluid system's
internal temperature [11].

Thus, the focus of this study is to find a different approach to solving the nanofluid flow problem to the stretching and shrinking surfaces while investigating it with MATLAB's BVP4C.

2. Methodology

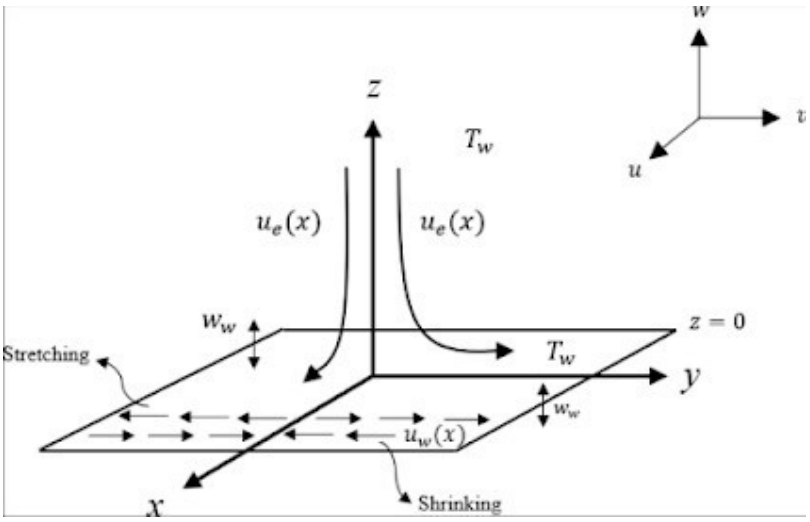

Figure 1: Physical model of stretching/shrinking surface

The figure above illustrates the model of the study that uses several variables and notations that have their own value and effect. The stretching and shrinking sheet denoted as $u_w(x)$ while

$u_e(x)$ is the outward flow velocity of the nanofluid with the constant c, where $c > 0$ is for the stretching surface while $c < 0$ for the shrinking surface [13]. Based on Figure 1, moving outward-pointing arrows show the surface is stretching, while inward-pointing arrows show the shrinking surface. On the other hand, the velocity of mass flux is denoted as w_w . The injection of mass flux occurs when $w_w > 0$ while $w_w < 0$ for suction. Next, the notation of T_w is the temperature of fluid in the boundary layer since this researcher used different fluids which are water-based either copper (Cu) or silver (Ag). Hence,

The continuity equation is governed by,

$$\frac{\partial u}{\partial x} + \frac{\partial v}{\partial y} + \frac{\partial w}{\partial z} = 0 \tag{1}$$

The momentum equation is,

$$u\frac{\partial u}{\partial x} + v\frac{\partial u}{\partial y} + w\frac{\partial u}{\partial z} = u_e\frac{\partial u_e}{\partial x} + v_{nf}\frac{\partial^2 u}{\partial z^2} \tag{2}$$

Energy equation governed by,

$$u\frac{\partial T}{\partial x} + u\frac{\partial T}{\partial x} + u\frac{\partial T}{\partial x} = \alpha_{nf}\frac{\partial^2 T}{\partial z^2} \tag{3}$$

and the boundary conditions are

$$\begin{aligned} &u = u_w(x) = ax, \quad v = 0, \quad w = w_w, \quad T = T_w \quad at\ z = 0 \\ &u = u_e(x) = cx, \quad T = T_\infty \quad at\ z = \infty \end{aligned} \tag{4}$$

where variable u and v are the components of x and y velocity respectively, $u_w(x) = ax$ is referred to shrinking/stretching velocity and $u_e(x) = cx$ denoted as the velocity of nanofluid external flow. This parameter will stretch the surface if the value of $c > 0$ while shrinking is $c < 0$. Then, w_w denoted as the velocity of mass flux , where it is injection when the condition $w_w > 0$ and suction when $w_w < 0$. The use of the parameter T represents temperature where T_w is the surface temperature and T_∞ is the temperature of the fluid far away from the surface. Therefore,

The similarity equation variables given by

$$u = cf'(\eta)\,, \qquad v = c(m-1)yf'(\eta), \qquad w = -\sqrt{cv}\,mf(\eta)$$
$$\theta(\eta) = \frac{T - T_\infty}{T_w - T_\infty}, \qquad \eta = \sqrt{\frac{c}{v}}\,z \tag{5}$$

In this case, $m = 1$ represents a single direction of shrinking sheet and $m = 2$ an asymmetric shrinkage. Hence, by using a similarity transformation, the differentiated variable will be substituted into (1), (2), and (3) to obtain the ODE as below

$$k_1 f''' + mf\,f'' + 1 - f'^2 = 0 \tag{6}$$

and

$$k_2\,\theta'' + Prmf\,\theta' = 0 \tag{7}$$

with boundary condition as follows

$$f(0) = s,\ f'(0) = \lambda,\ \theta(0) = 1,\ f'(\eta) \to 1,\ \theta(\eta) \to 0 \quad as\ \eta \to \infty \tag{8}$$

where k_1, k_2, the Prandtl number (Pr), shrinking and stretching parameter (λ) and suction parameter (s) are defined as:

$$k_1 = \frac{1}{(1-\phi)^{2.5}\left(\frac{1-\phi+\phi\rho_s}{\rho_f}\right)}, \quad k_2 = \frac{k_{nf}/k_f}{(1-\phi)+\left(\frac{\phi(\rho C_\rho)_s}{(\rho C_\rho)_f}\right)}, \tag{9}$$

$$Pr = \frac{v_f}{\alpha_f}, \quad s = -\frac{w_w}{(cv)^{\frac{1}{2}}}, \quad \lambda = \frac{\alpha}{c}, \tag{10}$$

where the suction parameter is stretching when $\lambda > 0$ while shrinking $\lambda < 0$.

This study only focuses on two physical quantities, which are the skin friction coefficient, C_f and the local Nusselt number, Nu_x which both of which can be written as equation below:

$$Re_x^{\frac{1}{2}} C_f = \frac{1}{(1-\phi)^{2.5}} f''(0), \quad Re_x^{-\frac{1}{2}} Nu_x = -\frac{k_{nf}}{k_f}\theta'(0) \tag{11}$$

where the dimensionless parameter of Reynolds number as $Re_x = \frac{u_e(x)x}{v}$. The effective viscosity and thermal diffusivity of nanofluid. Hence, the variable was given as below.

$$\mu_{nf} = \frac{\mu_f}{(1-\phi)^{2.5}}, \quad \alpha_{nf} = \frac{k_{nf}}{\left(\rho C_\rho\right)}, \quad \frac{k_{nf}}{k_f} = \frac{k_s + 2k_f - 2\phi\left(k_f - k_s\right)}{k_s + 2k_f - \phi\left(k_f - k_s\right)} \tag{12}$$

and

$$\left(\rho C_\rho\right)_{nf} = (1-\phi)\left(\rho C_\rho\right)_f + \phi\left(\rho C_\rho\right)_{s,} \quad \rho_{nf} = (1-\phi)_{\rho f} + \phi\rho_s. \tag{13}$$

3. Result and discussion

The results are compared with two previous findings by [13], who applied the shooting method with Runge-Kutta Fehlberg in Maple and [12], who solved the problem numerically using another method. This comparison aims to confirm that the results generated by BVP4C are valid. Table 1 represents the comparison results for skin friction coefficient, $f''(0)$, when $s = 0,\ \phi = 0$ with various of λ for Cu nanoparticle with $m = 1, 2$. While Table 2 presents the comparison of the value local Nusselt number for Cu nanoparticle with $m = 2, s = 0.5$ and various of λ.

Table 1: The comparison of value skin friction coefficient $f''(0)$ for Cu nanoparticle with $m = 1, 2$ (the sheet shrink at one direction and asymmetrically) $s = 0, \phi = 0$ and various of λ.

λ	[13]		[12]		Present study	
	$m = 1$	$m = 2$	$m = 1$	$m = 2$	$m = 1$	$m = 2$
1	0	0	0	0	0	0
0.5	-	-	0.1733	0.78032	0.7133	0.78032
0	1.232588	1.311938	1.232588	1.311938	1.232588	1.311938
-0.5	-	-	1.49567	1.49001	1.49567	1.49001
-0.75	-	-	1.49567	1.49001	1.49567	1.49001

Table 2: The comparison of local Nusselt number for Cu nanoparticle with $m = 2, s = 0.5$ and various of λ.

λ	[12]		Present study	
	$\phi = 0$	$\phi = 0.1$	$\phi = 0$	$\phi = 0.1$
1	8.2292	6.3563	8.2292	6.3563
0.5	7.7302	5.9489	7.7302	5.9489
0	7.1440	5.4757	7.1440	5.4757
-0.5	6.4033	4.8927	6.4033	4.8927
-0.75	5.9206	4.5291	5.9206	4.5291

Based on the table comparison of Table 1 and Table 2 the value of skin friction and Nusselt number obtained as previous study. Thus, this indicates that the present study is consistent with the previous research even though the method used is different. The previous study obtained the result by using shooting method whereas the present study used BVP4C method. Hence, the research satisfies the agreement.

3.1 Effect of shrinking/stretching parameter, λ on velocity profile and temperature profile, skin friction coefficient and local Nusselt number.

According to Figure 3.1 and Figure 3.2, it shows the different values of λ on temperature and velocity profile respectively. Figure 3.1 represents the velocity profile graft while Figure 3.2 representes the temperature profile with different values of stretching/shrinking value of λ. The negative value of $\lambda = -1.5, -1.6$ shows there exists a second solution which is considered as shrinking cases while there is no dual solution in the stretching case. Hence, the velocity profile illustrates that the stretching case increases steadily as it approaches 1. This reduces the thickness of the boundary layer. While Figure 3.2 demonstrates that the temperature profile declines with different values of lambda. However, stretching generates a reduction in the boundary layer as heat transfer from the surface to the fluid increases.

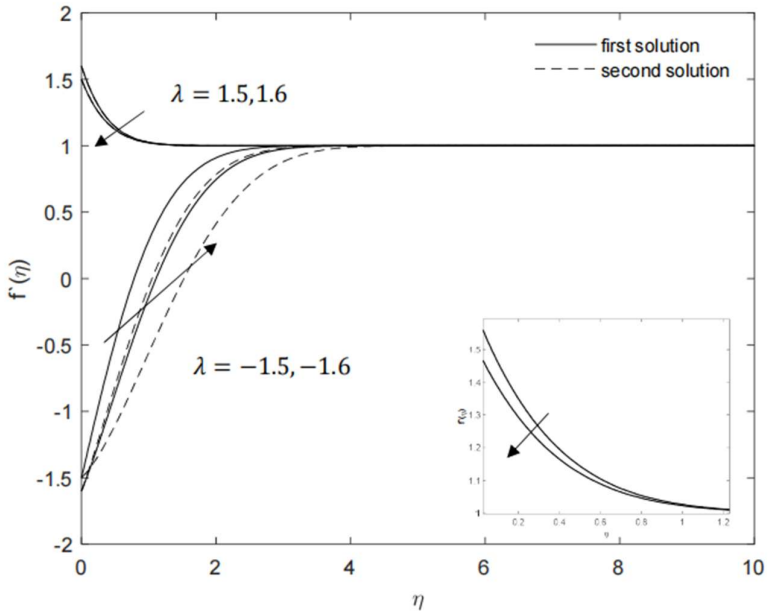

Figure 3.1: The velocity profile for different types of stretching/shrinking parameter $\lambda = 1.5,1.6,-1.5,-1.6$ with $m = 1, s = 0.5$ (permeable).

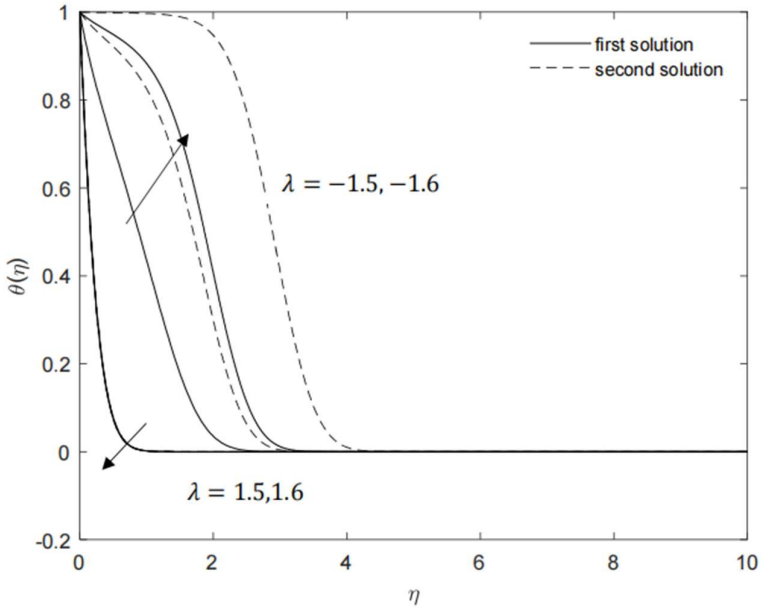

Figure 3.2: The temperature profile for different types of stretching/shrinking parameter $\lambda = 1.5,1.6,-1.5,-1.6$ with $m = 1, s = 0.5$.

Figure 3.3 and Figure 3.4 below illustrate the graph of skin friction coefficient and local Nusselt number that shows the dual solution exists based on the profile graph above. Figure 3.3 shows that for $\lambda > 1$, as the rise of the suction parameter s contributes to a higher value of the skin friction coefficient, thus it is indicated that the suction delays the boundary layer separation.

While Figure 3.4, the increase of local Nusselt number as suction parameter also increases where λ is decreases. Thus, it is illustrated that the suction delayed separation of boundary layer. In addition, both Figure 3.3 and Figure 3.4 demonstrate that the second solution exists in $s = 0.5, 0.6, 0.7$. A difference in the stretching/shrinking parameter, λ indicates the existence of the second solution where it only exists at the negative value for all values of s which shows it exist in the shrinking cases but not in stretching cases.

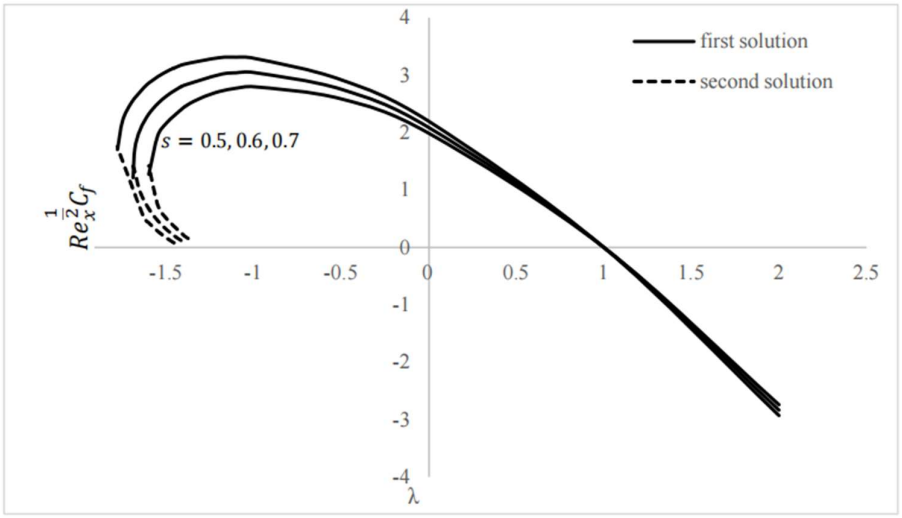

Figure 3.3: The Skin friction coefficient, $Re_x^{\frac{1}{2}} C_f$ versus λ with different type suction parameter, $s = 0.5, 0.6, 0.7$ when $m = 1, \phi = 0.1$.

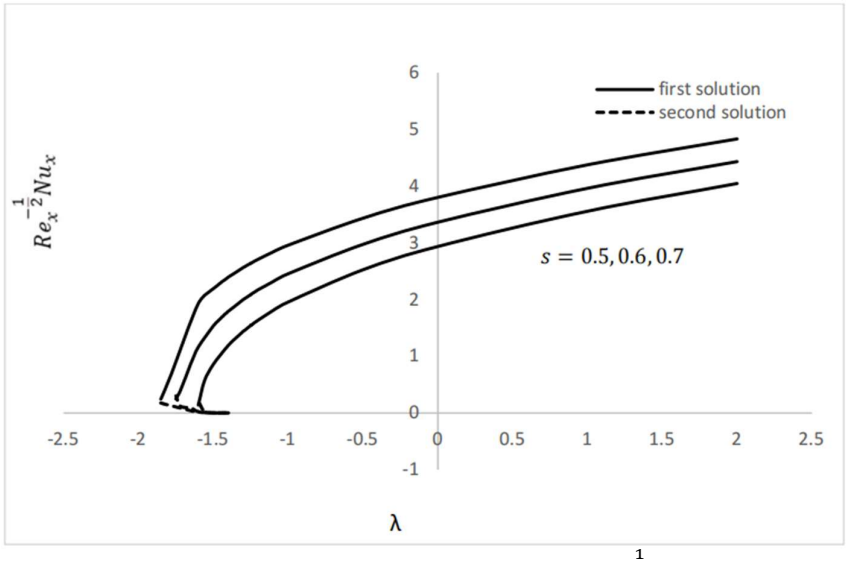

Figure 3.4: Variation of local Nusselt number, $Re_x^{-\frac{1}{2}} Nu_x$ versus λ for Ag nanoparticle when $m = 1, \phi = 0.1$ and various value of s

3.2 Effect of different types of nanoparticles (copper and silver) on skin friction coefficient and local Nusselt number.

The skin friction coefficient and local Nusselt number versus λ with different types of nanoparticles (Cu, Ag) when $m = 1, \phi = 0.1, s = 0.5$ were shown in Figure 3.5 and Figure 3.6 below. From Figures 3.5 and 3.6 there exist regions with unique solutions for $\lambda > -1$, dual solutions for $\lambda_c < \lambda < -1$, and no solutions for $\lambda < \lambda_c$, where λ_c represents the critical value of λ. It is demonstrated that as λ drops, the skin friction coefficient increases and the local Nusselt number decreases. Therefore, Figure 3.6 shows the local Nusselt number for copper and silver decreases as lambda decreases. The transfer of heat from the fluid's surface is measured by the Nusselt number where increased Nusselt number, enhanced heat transportation, and reduced thermal boundary layer thickness.

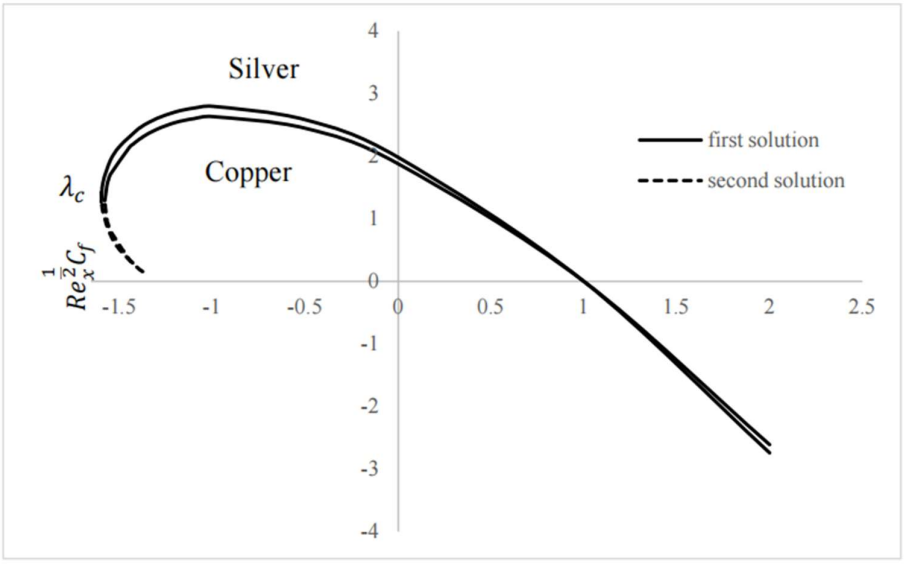

Figure 3.5: The Skin Friction Coefficient, $Re_x^{\frac{1}{2}}C_f$ versus λ with different type nanoparticle(Cu, Ag), $m = 1, \phi = 0.1, s = 0.5$.

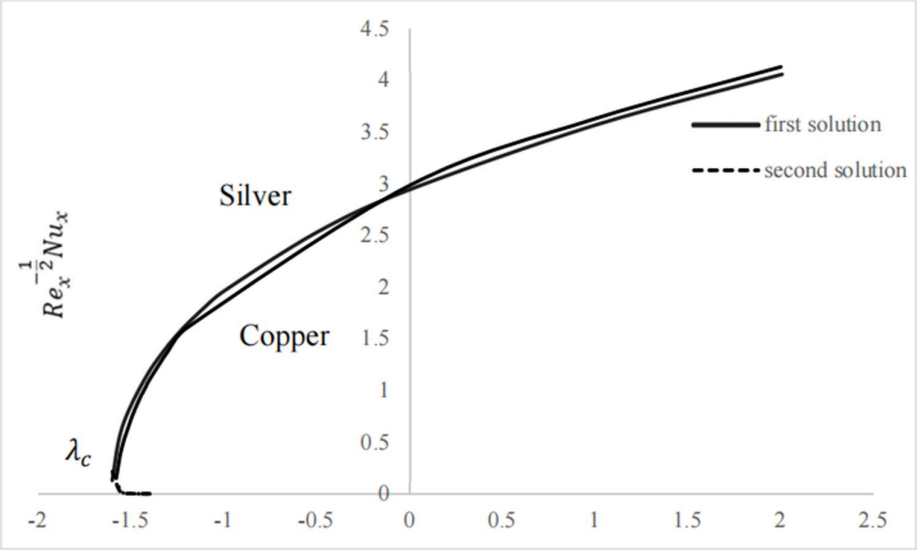

Figure 3.6: Local Nusselt number, $Re_x^{-\frac{1}{2}}Nu_x$ versus λ for different type nanoparticles (Cu, Ag) when $m = 1, \phi = 0.1\ s = 0.5$.

4. Conclusion

The purpose of this study is to investigate nanofluid flow over a permeable stretching and shrinking surface. Similarity reduction variables are used to transform the nonlinear partial differential equations (PDEs) into ordinary differential equations (ODEs). The equations are then numerically solved using MATLAB's built-in BVP4C solver. The results are compared with previous research to validate the accuracy of BVP4C. The findings confirm the validity of the results, as they had a good agreement with the earlier studies. Additionally, this study analyses the influence of stretching/shrinking parameters and the suction parameter on the velocity and temperature profiles, as well as the effect of copper and silver nanoparticles on the skin friction coefficient and local Nusselt number.

5. Acknowledgments

The authors would like to thank the Faculty of Computer Science and Mathematics, Universiti Teknologi Mara, Dr. Siti Hidayah Binti Muhad Saleh as supervisor for the support.

6. References

[1] Sreelakshmy K.R, Nair, A. S.,& Nair, S. C. (2014). Av overview of recent research. *International Research Journal Of Pharmacy*, *5*(4), 239–243. https://doi.org/10.7897/2230-8407.050451

[2] Wahid, N. S., Arifin, N. M., Khashi'ie, N. S., & Pop, I. (2023). Three-dimensional unsteady radiative hybrid nanofluid flow through a porous space over a permeable shrinking surface. *Chinese Journal of Physics*, *85*, 196–211. https://doi.org/10.1016/j.cjph.2023.07.016

[3] Zaimi, K., & Ishak, A. (2015). Boundary layer flow and heat transfer over a permeable stretching/shrinking sheet with a convective boundary condition. *Journal of Applied Fluid Mechanics*, *8*(3), 499–505. https://doi.org/10.18869/acadpub.jafm.67.222.22793

[4] Yahaya, R. I., Mustafa, M. S., Md Arifin, N., Pop, I., Md Ali, F., & Mohamed Isa, S. S. P. (2023). Hybrid nanofluid flow past a biaxial stretching/shrinking permeable surface with radiation effect: Stability analysis and heat transfer optimization. *Chinese Journal of Physics*, *85*, 402–420. https://doi.org/10.1016/j.cjph.2023.06.003

[5] Patil, P. M., Kulkarni, M., & Hiremath, P. S. (2020). Effects of surface roughness on mixed convective nanofluid flow past an exponentially stretching permeable surface. *Chinese Journal of Physics*, *64*, 203–218. https://doi.org/10.1016/j.cjph.2019.12.006

[6] Konai, S., & Mukhopadhyay, S. (2024). Nanofluid flow past a nonlinearly stretched surface with shear flow and zero nanoparticle flux. *Partial Differential Equations in Applied Mathematics*, *9*. https://doi.org/10.1016/j.padiff.2024.100643

[7] Idris, S., Jamaludin, A., Nazar, R., & Pop, I. (2023). Radiative MHD flow of hybrid nanofluid over permeable moving plate with Joule heating and thermal slip effects. *Alexandria Engineering Journal*, *83*, 222–233. https://doi.org/10.1016/j.aej.2023.09.065

[8] Patel, V. K., Pandya, J. U., & Patel, M. R. (2023). Testing the influence of TiO2− Ag/water on hybrid nanofluid MHD flow with effect of radiation and slip conditions over exponentially stretching & shrinking sheets. *Journal of Magnetism and Magnetic Materials*, *572*. https://doi.org/10.1016/j.jmmm.2023.170591

[9] Zainal, N. A., Nazar, R., Naganthran, K., & Pop, I. (2021). Unsteady MHD stagnation point flow induced by exponentially permeable stretching/shrinking sheet of hybrid nanofluid. *Engineering Science and Technology, an International Journal*, *24*(5), 1201–1210. https://doi.org/10.1016/j.jestch.2021.01.018

[10] Khan, U., Waini, I., Ishak, A., & Pop, I. (2021). Unsteady hybrid nanofluid flow over a radially permeable shrinking/stretching surface. *Journal of Molecular Liquids*, *331*. https://doi.org/10.1016/j.molliq.2021.115752

[11] Wahid, N. S., Arifin, N. M., Yahaya, R. I., Khashi'ie, N. S., & Pop, I. (2024). Impact of suction and thermal radiation on unsteady ternary hybrid nanofluid flow over a biaxial shrinking sheet. *Alexandria Engineering Journal*, *96*, 132–141. https://doi.org/10.1016/j.aej.2024.03.079

[12] Arifin, N. M., Nazar, R., & Pop, I. (2011). Viscous flow due to a permeable stretching/shrinking sheet in a nanofluid. *Sains Malaysiana*, *40*(12), 1359-1367. https://core.ac.uk/download/pdf/11492130.pdf

[13] Ismail, N. H., & Aman, F. (2023). Solving Nanofluid Flow Over a Permeable Stretching and Shrinking Surfaces using Shooting Technique. *Enhanced Knowledge in Sciences and Technology*, *3*(1), 064-069.
https://penerbit.uthm.edu.my/periodicals/index.php/ekst/article/view/10309